

Pr₁₂I₁₇Fe₂: A Novel Hypostoichiometric Compound with Only Isolated Clusters

Younbong Park and John D. Corbett*

Department of Chemistry, Iowa State University, Ames, Iowa 50011-3020

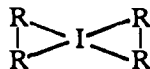
Received August 11, 1993*

Reactions of the elements with PrI₃ in sealed Nb containers at 860–920 °C yields Pr₁₂I₁₇Z₂ for Z = Fe and Re. The new structure type was characterized for the former (P $\bar{1}$, Z = 1, *a* = 11.798 (4) Å, *b* = 11.791 (2) Å, *c* = 9.830 (2) Å, α = 114.87(2)°, β = 104.82(4)°, γ = 93.19(2)°, *R*/*R*_w = 3.2/3.8% for 2967 data, 143 variables). The unusually low I:Pr ratio for a phase with isolated clusters is achieved by seven I⁻ⁱ bridges per cluster in which iodine simultaneously bridges metal edges in two clusters. The Z-centered Pr₆I₁₂-type clusters are joined into layers by three pairs of centric I⁻ⁱ and (I^{-a}) bridges. The layers are further joined in the third direction by a unique planar I⁻ⁱ plus other types of iodine bridges. The 2.75-Å Pr–Fe bonds appear to be particularly short.

Introduction

A considerable variety of condensed rare-earth-metal (R) iodide clusters have been discovered in recent years that are derived from R₆I₁₂ units and centered by late transition metals. Although the metal frameworks in all of these consist of rare-earth-metal octahedra sharing edges, the members encompass tetrameric oligomers, infinite chains, three-dimensional arrays, and double metal sheets of condensed clusters, each of which are interconnected via shared iodine atoms.^{1,2} No cluster of the rare-earth elements (R) or Zr is known to lack the evidently essential interstitial.

Recently, there have been several interesting examples in which the interstitial atoms (Z) in Gd₃I₃Mn double chains, Gd₅I₇Mn oligomers,³ and Y₂Br₇Fe_{2+x} double layers⁴ exhibit particularly short contacts with like neighbors that lead to novel structural distortions or even to new structural frameworks. It is striking that these have been found only with the 3d element interstitials, while many heavier transition-metal analogues afford more regular structures with weaker Z–Z interactions. This has prompted us to investigate systems containing 3d interstitials in more extensive ways, even though many members have been well studied and characterized before.^{5–8} Our efforts in the Pr–I–Fe systems have yielded another novel three-dimensional compound, Pr₁₂I₁₇Fe₂. Even though short interstitial–interstitial interactions are not observed, the result is, to our knowledge, the halogen-poorest phase in which clusters are joined only through bridging iodides, as opposed to via shared edges of R₆ cluster octahedra. The R:I ratio of the title compound is equal to that of Gd₁₂I₁₇C₆, but the latter consists solely of Gd₆ octahedral clusters with acetylide interstitials that share metal edges to form chains.⁹ In the present case, the low iodine content is secured by extensive intercluster bridging by I⁻ⁱ functions, that is, through iodine that bridges metal edges on two separate cluster units, viz.,



but not necessarily in a planar manner.

Experimental Section

Syntheses. All reactions were carried out as before^{5–7} in welded 3/8-in. diameter Nb tubes within well-baked silica jackets. Pr, sublimed PrI₃, and elemental Mn, Fe, Co, Ni, Ru, Rh, Re, Os, Ir, Pt, and Au were investigated on ~200-mg scales for a variety of stoichiometries and reaction temperatures. Product distributions were estimated from Guinier powder pattern intensities. The 70% yields of the title phase are obtained at 860–920 °C in 10–14 d from somewhat Fe-rich compositions. Competitive phases are Pr₇I₁₂Fe,⁶ when the system is somewhat more oxidized (iodine rich), and Pr₂IFe₂ (Gd₂IFe₂ type⁴), especially for even Fe-richer systems. The same Pr₁₂I₁₇Fe₂ was found to be present in 80–95% yields in previously unknown powder patterns of products obtained by two earlier investigators when working at 850–925 °C with target compositions near Pr₃I₃Fe (28 d). The new structure has also been found for Pr₁₂I₁₇Re₂ that forms along with Pr₇I₁₂Re⁶ from reactions of Pr₄I₅Re compositions at 920 °C. On-stoichiometry reactions give largely Pr₇I₁₂Re instead, probably because the inevitable PrOI formation from adventitious sources (water slowly evolved from the silica jacket, most likely) leaves the system more oxidized. The Guinier-based lattice constants for the Re compound are *a* = 11.770(9) Å, *b* = 11.870(3) Å, *c* = 9.835(4) Å, α = 104.90(2)°, β = 114.29(3)°, γ = 93.20(3)°, and *V* = 1190(1) Å³.

The new phase was once thought to occur with Mn as well, and the crystal structure of “Pr₁₂I₁₇Mn₂” was first solved for one of a few crystals found after an evidently errant reaction at 920 °C. The major product was PrOI, likely exacerbated by contaminated Pr and Mn, plus PrI₂ and Mn. Many subsequent variations of reactants proportions and conditions have not enabled a direct synthesis of any discernible amount of the supposed compound, gaining rather Pr₇I₁₂Mn,⁶ PrI₂, Pr₂I₅, and Mn in various mixtures. We have concluded that the structure solution for an insignificantly larger cell (1177.3(5) Å³ from the diffractometer) pertained to a product stabilized by unknown and possibly mixed impurities. Addition of PrH₃ did not help, and the phase did not form with La either.

Because of the 17.5 e⁻/cluster present in Pr₁₂I₁₇Fe₂ (see Results) and 16.5 e⁻ in the once-believed Mn analogue, some efforts were made to prepare mixed interstitial, 17-e⁻ examples. Reactions at 890 °C with Mn and Ru gave Pr₇I₁₂Ru plus Mn, while Fe and Re gave a good yield of Pr₁₂I₁₇Fe₂, elemental Re, and small amounts of unknowns. The interstitial identity of this iron product was established by crystallography and by an SEM–EDS study of nine crystals which detected Fe but no Re.

Reactions with Ni, Ru, Rh, Os, Ir, Pt, and Au did not stabilize any Pr₁₂I₁₇Z₂ products although some of these did afford new cubic Pr₃I₃Au, monoclinic Pr₃I₃Os, Pr₂INi₂ (Gd₂IFe₂ type⁴),⁸ and several unknown phases that are still under investigation.

The course of these exploratory reactions, especially the extensive unsuccessful ones carried out with Mn, did indicate a means whereby the inevitable oxyhalide contamination could be ameliorated. These ROX

* Abstract published in *Advance ACS Abstracts*, March 15, 1994.

- (1) Simon, A.; Mattausch, H.J.; Miller, G. J.; Bauhofer, W.; Kremer, R. K. In *Handbook on the Physics and Chemistry of Rare Earths*; Gschneidner, K. A., Eyring, L., Eds.; Elsevier Science Publishers: North-Holland, The Netherlands, 1991; Vol. 15, p 191 and references therein.
- (2) Corbett, J. D. In *Modern Perspectives in Inorganic Chemistry*; Parthe, E., Ed.; Kluwer Academic Publishers: Dordrecht, The Netherlands, 1992; p 27 and references therein.
- (3) Ebihara, M.; Martin, J. D.; Corbett, J. D. *Inorg. Chem.*, in press.
- (4) Ruck, M.; Simon, A. *Z. Anorg. Allg. Chem.* **1993**, *619*, 327.

(5) Hughbanks, T.; Corbett, J. D. *Inorg. Chem.* **1988**, *27*, 2022.

(6) Payne, M. W.; Corbett, J. D. *Inorg. Chem.* **1990**, *29*, 2246.

(7) Payne, M. W.; Dorhout, P. K.; Corbett, J. D. *Inorg. Chem.* **1991**, *30*, 1467.

(8) Park, Y.; Corbett, J. D. To be submitted for publication.

(9) Simon, A.; Warkentin, E. *Z. Anorg. Allg. Chem.* **1983**, *497*, 79.

Table 1. Data Collection and Refinement Parameters for Pr₁₂I₁₇Fe₂

lattice params ^a	space group, Z	P1̄ (No. 2), 1
a, Å	11.798(4)	μ(Mo Kα), cm ⁻¹
b, Å	11.791(2)	transm factors (scaled)
c, Å	9.830(2)	no. indep refl, variables
α, deg	114.87(2)	R/R _w ^b %
β, deg	104.82(4)	
γ, deg	93.19(2)	
V, Å ³	1178.4(5)	

^a Guinier data with Si as an internal standard, λ = 1.540 562 Å, 22 °C. ^b $R = \sum ||F_o| - |F_c|| / \sum |F_o|$; $R_w = [\sum w(|F_o| - |F_c|)^2 / \sum w(F_o)^2]^{1/2}$, $w = \sigma_F^{-2}$.

phases arise not just from usually small amounts of oxide in the reagents but largely from water that slowly diffuses out the fused silica jackets and through the Nb walls over several weeks, especially above about 850 °C. Gettering of oxygen by excess R metal is not a solution since ROX formation (from R(O) and RX₃) has been shown to be a good means to remove oxide from these and other metals.¹⁰ As a result, when several R, RI₃ reactions with different Z are run in separate Nb containers sealed within the same jacket, those that do not yield interstitially-stabilized products and therefore have higher RI₃ activities are observed to suffer the larger contamination with ROI. Thus an internal gettering, even with just RI₃ in one container, would appear to be profitable.

Single-Crystal X-ray Study. A black rectangular crystal ca. 0.04 × 0.08 × 0.17 mm of "Pr₁₂I₁₇Mn₂" (see above) was mounted in a thin-walled capillary in the glovebox. Triclinic cell parameters were obtained on a Rigaku AFC6R diffractometer from the least-squares refinement of the four axial settings of 25 machine-centered reflections. Diffraction data were collected at room temperature with the aid of graphite-monochromated Mo Kα radiation and an ω-2θ scan mode. The stability of the experimental setup and the crystal integrity were monitored with three standard reflections that were measured every 150 reflections during data collection. The intensities did not show any appreciable change. Empirical absorption corrections based on the average of three ψ scans at different values of θ were applied to the entire data set. All atoms in the structure were found in space group P1̄ with the aid of direct methods (SHELXS-86¹¹). The set was transformed to P1̄ with a proper choice of origin and was refined with the TEXSAN¹² package of programs on a VAX station 4000 computer. All atoms were refined anisotropically. The least-squares refinement converged smoothly to R(F)/R_w values of 2.4/2.8%.

When production of a good yield of the supposed Mn example proved impossible, a full sphere of room-temperature diffraction data to 2θ = 50° was collected from a larger crystal of Pr₁₂I₁₇Fe₂ on the same diffractometer. This gave 24% more observed unique reflections and a routine refinement to R/R_w = 3.2/3.8%. The parameter errors were now somewhat less, the metal ellipsoids smaller, and the metal cluster a little smaller and more regular. The iron occupancy refined to 102(1)%. The largest residual in the final difference map was 1.29 e/Å³ that was located about 1.25 Å from Pr4. Some data collection and refinement parameters are given in Table 1. The final atomic coordinates, isotropic-equivalent temperature factors and their estimated standard deviations are listed in Table 2. A larger summary of collection and refinement information as well as anisotropic displacement parameters for all atoms are tabulated in the supplementary material. Structure factor data are available from J.D.C.

Results and Discussion

The structure of Pr₁₂I₁₇Fe₂ features a quite complicated three-dimensional framework constructed from Pr₆I₁₂ octahedral clusters centered by Fe interstitials. The complexities are necessary in order to harmonize the iodine hypostoichiometry with the evidently fundamental bonding requirements of such octahedral clusters, namely, that all 12 edges be bridged by inner (i) iodine and that all 6 vertices be bonded to an exo (a) iodine, i.e., M₆I₁₂I₆^a in the isolated case.² Because of the low I:Pr ratio relative to that of the Pr₆I₁₂Fe units, there is a need for many shared, bifunctional (even trifunctional) iodine atoms. In the

Table 2. Positional Parameters and B(eq) Values (Å²) for Pr₁₂I₁₇Fe₂

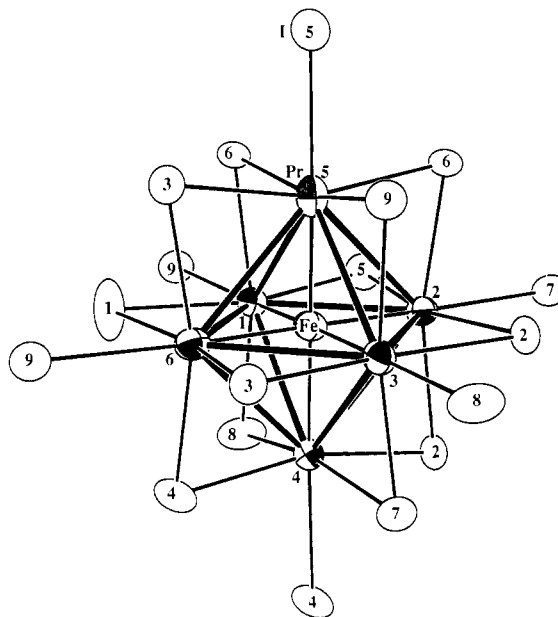
atom	x	y	z	B(eq) ^a
Pr1	0.15167(6)	0.28826(7)	0.15334(8)	1.32(3)
Pr2	0.32622(6)	0.51498(7)	0.06198(8)	1.33(3)
Pr3	0.28422(6)	0.23921(7)	0.64152(7)	1.30(2)
Pr4	0.42023(6)	0.18701(7)	0.00860(8)	1.29(3)
Pr5	0.00750(6)	0.33365(7)	0.77891(8)	1.41(3)
Pr6	0.10433(6)	0.01102(7)	0.73484(8)	1.36(3)
I1	0	0	0	2.95(6)
I2	0.41335(7)	0.53062(8)	0.7767(1)	1.63(3)
I3	0.16400(7)	0.94328(8)	0.4067(1)	1.70(3)
I4	0.32224(8)	0.88740(9)	0.83	1.81(4)
I5	0.24792(8)	0.58636(8)	0.3724(1)	1.81(4)
I6	0.10872(7)	0.63902(8)	0.9415(1)	1.66(3)
I7	0.45813(7)	0.2102(1)	0.3298(1)	2.55(4)
I9	0.04518(7)	0.30147(9)	0.4514(1)	1.76(3)
Fe	0.2147(1)	0.2622(2)	0.8951(2)	0.81(5)

^a $B(\text{eq}) = (8\pi^2/3) \sum_i \sum_j U_{ij} a_i^* a_j^* \tilde{a}_i \tilde{a}_j$.

Table 3. Iodine Functionality in Pr₁₂I₁₇Fe₂

iodine	bonding mode	CN	geometry
1	i-i	4	rectangular
2	i-i	4	seesaw ^a
3	i-i	4	seesaw
4	i-a	3	~planar
5	i-a	3	trig pyramidal
6	i-i	4	seesaw
7	i-a	3	trig. pyramidal
8	i-a	3	~planar
9	i-a-a	4	~tetrahedral

^a Distorted tetrahedron, ~C_{2v}.

**Figure 1.** The one type of cluster in Pr₁₂I₁₇Fe₂ with the atom-numbering scheme (90% probability thermal ellipsoids).

present case, each cluster has seven inner iodines that bridge edges of and join two clusters (Iⁱ⁻ⁱ), four more that bridge one edge and are exo to a vertex in another cluster (I^{i-a}), and one that adds yet a second vertex to its bonding (I^{i-a-a}). The cluster can then be written as Pr₆(Fe)(Iⁱ⁻ⁱ)_{7/2}(I^{i-a})₄I^{i-a-a} = Pr₆I_{8.5}Fe. Table 3 relates the numbering of all iodines to their functionality and geometry for future reference.

Even with this complex nature, the structure can be developed from layers of Iⁱ⁻ⁱ-bridged clusters that are then connected to each other to form the three-dimensional framework. All clusters are equivalent and related either by translation or inversion. Figure 1 shows the numbering system in a single cluster, and Figure 2 illustrates the bridging of each cluster to three others in the same

(10) Corbett, J. D.; Smith, J. D.; Garcia, E. J. *Less-Common Met.* **1986**, *115*, 343.

(11) Sheldrick, G. M. SHELXS-86. Universität Göttingen, BRD, 1986.

(12) Texray Structure Analysis Package, Molecular Structure Corp., The Woodlands, TX, 1985.

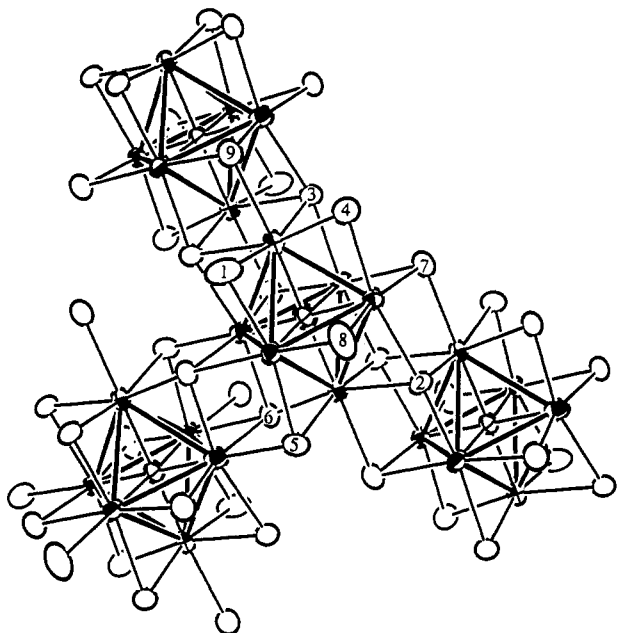


Figure 2. Three independent bridges between clusters in Pr₁₂I₁₇Fe₂ each consisting of pairs of Iⁱ⁻ⁱ (12, 13, or 16) and I^{i-a} (17, 19, or 15, respectively) about an inversion center. The view is approximately along [00 $\bar{1}$].

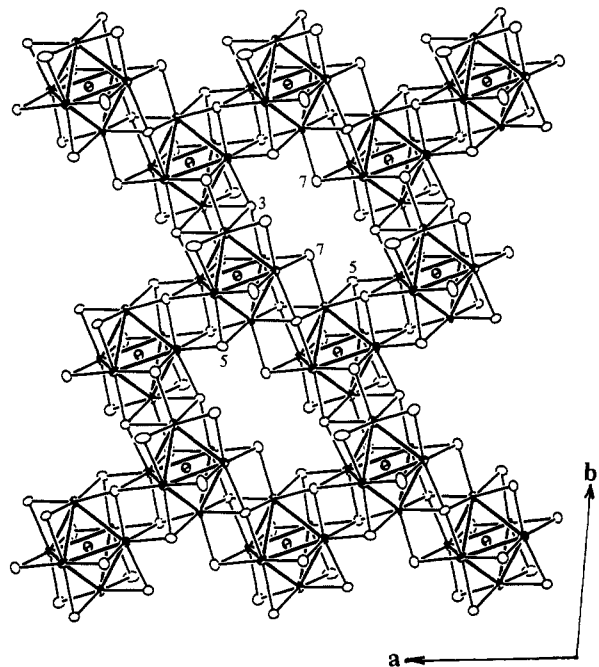


Figure 3. Layers generated by the bridging modes shown in Figure 2. One of the three zigzag chain choices lies across the bottom of the figure.

layer as viewed along a quasi 3-fold axis. Each bridge consists of a distinctive pair of Iⁱ⁻ⁱ (12, 13, or 16, as labeled) functions together with a pair of opposed I^{i-a} and I^{a-i} bridges about these (17, 19, 15, respectively) that lie roughly normal to the adjoining Iⁱ⁻ⁱ pair with respect to the intercluster axis. Each group of these four-atom bridges surrounds a center of symmetry that lies on the body center, the *c* edge, or the *bc* face of the unit cell, respectively. This four-atom bridging scheme was first seen in Y₆I₁₀Ru where pairs of these are trans across each cluster and generate linear chains.¹³

The essence of the overall intralayer bonding so generated in Pr₁₂I₁₇Fe₂ is seen in Figure 3 where six-rings of bridged clusters are evident. With structural similarity in mind, one can visualize

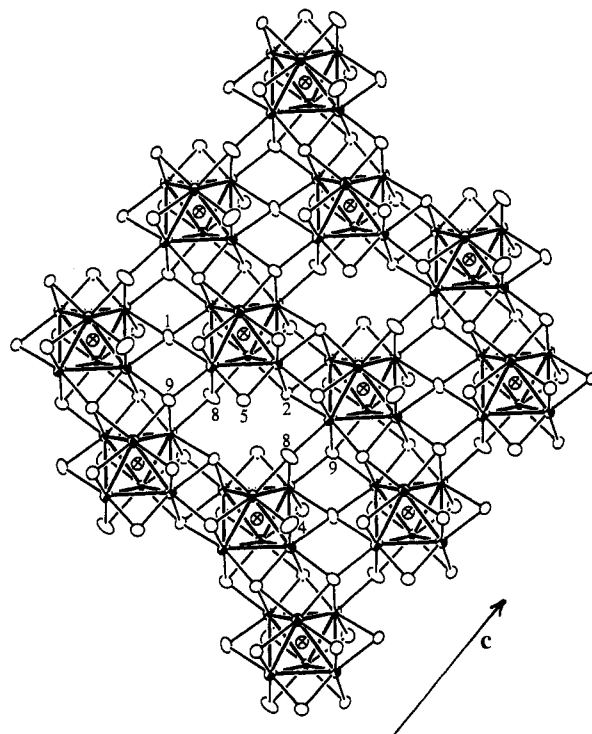


Figure 4. Interlayer bridging via Iⁱ⁻ⁱ, I^{8i-a}, I^{4i-a} (only the I^a portion shown), and I^{9i-a-a}. The layers illustrated in Figure 3 are seen side-on from upper left to lower right (\sim [110]). Note the horizontal, approximately cubic-close-packed layers of I (and Fe) (90%).

this layer as composed of hypothetical one-dimensional chains like those in Y₆I₁₀Ru, one example of which lies across the bottom of Figure 3. (There are of course three choices of chains ca. 60° to one another.) These chains are different though as they run in a zigzag manner so as to join opposite faces on half of each octahedral cluster (i.e., square pyramids). The other half of each octahedron is used for additional interactions between parallel chains to form the layers. The joining of linear chains instead to gain this stoichiometry may be impossible because of severe I-I closed-shell contacts. The present structure seems unusual in that there is only one I...I contact below 4.20 Å (4.183 Å) in spite of the extensive sharing of iodine; *d*(I...I) values of 4.06 Å and even 4.00 Å are found in R₃I₃Z and others.

Since each octahedral Pr₆ cluster has three neighboring clusters in the layer bonded via six Iⁱ⁻ⁱ and three I^{i-a} atoms, the remaining three Iⁱ atoms per Pr₆I₁₂ cluster play roles in interlayer connections. Figure 4 shows these in a view parallel to the layers and approximately normal to that in Figure 3. The four special atoms here, 11, 4, 8, 9, are all labeled in Figure 2. The unique I¹¹ⁱ⁻ⁱ atom has planar geometry and connects each cluster in the layer to a fourth one in either the layer above or below. It lies on the inversion center 0,0,0 and therefore generates the half-integral stoichiometry per cluster. Two other iodine atoms, I⁸ and I⁴, have simple I^{i-a} bridging functions between the layers (the latter lies outside of the section in Figure 4). Finally, it will be noted in the figure that four-coordinate I⁹, which was already described as *i-a* within the layer (Figure 2), is also interlayer bonding to make it I^{i-a-a}. This is a new mode, although X^{a-a-a} examples are known.^{14,15} The two exo bonds that I⁹ forms, one intralayer, are 0.06 Å longer (3.44 Å, Table 4) than the average for exo bonds formed by three-coordinate I^{i-a}. The Pr-I⁹ⁱ bond lengths are similar to the four fairly short Pr-I bonds formed by Iⁱ⁻ⁱ, 3.248 Å average, while inner bonds for the three-coordinate I^{i-a} are the

(13) Hughbanks, T.; Corbett, J. D. *Inorg. Chem.* **1989**, *28*, 631.

(14) Ziebarth, R. P.; Corbett, J. D. *J. Am. Chem. Soc.* **1985**, *107*, 4571.
 (15) Sägebarth, M.; Simon, A. *Z. Anorg. Allg. Chem.* **1990**, *587*, 119.

Table 4. Selected Bond Distances (Å) and Angles (deg) in Pr₁₂I₁₇Fe₂ (Å)

1-2	distance	av	1-2	distance	av
Pr1-Pr2	3.814(2)		I1-Pr1(×2)	3.265(2)	
Pr1-Pr4	3.845(1)		I1-Pr6(×2)	3.199(1)	3.232
Pr1-Pr5	3.909(2)				
Pr1-Pr6	3.903(2)	3.868	I2-Pr2	3.293(1)	
Pr1-Fe	2.725(2)		I2-Pr2	3.264(1)	
			I2-Pr3	3.230(2)	
Pr2-Pr1	3.814(2)		I2-Pr4	3.261(2)	3.262
Pr2-Pr3	3.920(2)				
Pr2-Pr4	3.941(2)		I3-Pr3	3.243(2)	
Pr2-Pr5	3.899(1)	3.894	I3-Pr5	3.233(2)	
Pr2-Fe	2.767(2)		I3-Pr6	3.255(2)	
			I3-Pr6	3.289(1)	3.255
Pr3-Pr2	3.920(2)				
Pr3-Pr4	3.872(2)		I4-Pr4	3.194(2)	
Pr3-Pr5	3.888(1)		I4-Pr4	3.365(2)	
Pr3-Pr6	3.876(2)	3.889	I4-Pr6	3.179(2)	3.246
Pr3-Fe	2.732(2)				
			I5-Pr1	3.197(2)	
Pr4-Pr1	3.845(1)		I5-Pr2	3.201(1)	
Pr4-Pr2	3.941(2)		I5-Pr5	3.375(2)	3.258
Pr4-Pr3	3.872(2)				
Pr4-Pr6	3.840(1)	3.874	I6-Pr1	3.247(1)	
Pr4-Fe	2.756(2)		I6-Pr2	3.232(2)	
			I6-Pr5	3.263(2)	
			I6-Pr5	3.282(1)	3.256
Pr5-Pr1	3.909(2)		I7-Pr2	3.388(2)	
Pr5-Pr2	3.899(1)		I7-Pr3	3.196(1)	
Pr5-Pr3	3.888(1)		I7-Pr4	3.215(1)	3.266
Pr5-Pr6	3.914(2)	3.902			
Pr5-Fe	2.757(2)		I8-Pr1	3.176(2)	
			I8-Pr3	3.392(2)	
Pr6-Pr1	3.903(2)		I8-Pr4	3.236(2)	3.268
Pr6-Pr3	3.876(2)				
Pr6-Pr4	3.840(1)				
Pr6-Pr5	3.914(2)	3.883	I9-Pr1	3.422(1)	
Pr6-Fe	2.747(2)	2.747	I9-Pr3	3.267(2)	
			I9-Pr5	3.230(2)	
Pr6-Pr6	4.533(2)		I9-Pr6	3.463(2)	3.345
Pr5-Pr5	4.521(2)				
Pr2-Pr2	4.558(2)		I6-I9	4.188(2)	
1-2-3	angle	1-2-3	angle	1-2-3	angle
I9-Pr1-Fe	174.13(4)	Pr1-I1-Pr6(×2)	74.27(4)	Pr1-Fe-Pr6	91.01(7)
I7-Pr2-Fe	177.84(4)	Pr1-I1-Pr6(×2)	105.73(4)	Pr2-Fe-Pr3	90.95(7)
I8-Pr3-Fe	179.02(4)			Pr2-Fe-Pr4	91.04(6)
I4-Pr4-Fe	177.77(5)	Pr1-Fe-Pr3	178.40(6)	Pr2-Fe-Pr5	89.80(7)
I5-Pr5-Fe	178.44(5)	Pr2-Fe-Pr6	178.90(7)	Pr3-Fe-Pr4	89.73(7)
I9-Pr6-Fe	176.46(5)	Pr4-Fe-Pr5	179.16(8)	Pr3-Fe-Pr5	90.20(6)
		Pr1-Fe-Pr2	87.98(7)	Pr3-Fe-Pr6	90.06(7)
Pr1-I1-Pr1	180.00	Pr1-Fe-Pr4	88.10(5)	Pr4-Fe-Pr6	88.51(7)
Pr6-I1-Pr6	180.00	Pr1-Fe-Pr5	91.98(7)	Pr5-Fe-Pr6	90.65(6)

shortest, averaging 3.190 Å. The distances among the more usual iodine functionalities are typical in condensed cluster examples.^{5,16}

Horizontal close-packed layers of iodine-containing periodic Fe substitution to define cluster centers are clearly recognizable in Figure 4. These layers are cubic-close-packed in projection but they must be translated on repeat in order to generate the ladder-like cluster stacking shown.

There is one obvious correlation of iodine bridging functions with internal dimensions of the clusters: the long exo bond between the unusual four-coordinate I9 and Pr1 is opposite a short Pr1-Fe distance, 0.022 Å less than average. The angle Fe-Pr1-I9 is also the farthest from 180° (174.1°). General trends observed in the other systems² are that M-Z distances decrease as the opposed M-X^a distances increase and vice versa. This event occurs in other cases when the latter are increased by close-shell contacts (matrix effects) between I^a and the four adjoining Iⁱ at that vertex. The trans atoms are of course competing for some of the same metal orbitals.

(16) Payne, M. W.; Dorhout, P. K.; Kim, S.-J.; Hughbanks, T. R.; Corbett, J. D. *Inorg. Chem.* **1992**, *31*, 1389.

It is otherwise difficult to account for details of the (small) distortions of the Pr₆Fe unit in terms of Pr-I interactions in such a low-symmetry structure. The Pr-Fe bonds are elongated toward Pr2 and Pr4, which have the longest edge separation, but only by 0.02 Å. Most distortions are angular so as to give a Pr-Pr distance range of 0.125 Å. It is not yet clear whether the observed cluster distortions are associated in any way with electronic effects. The crystallographically equivalent clusters have average cluster-based counts of 17.5 e⁻, but there are no thermal ellipsoid effects that suggest a mixture of significantly different 17- and 18-e⁻ units are present. The degree of radial distortion is not as large as that seen in the centric 17-e⁻ clusters in Y₆I₁₀Ir₆ or Pr₆Br₁₀-Co,¹⁷ but these are unusual because of their chain structure.

The bonding to the source of the stabilization of this phase, Fe, again appears to be strong. The average *d*(Pr-Fe), 2.75 Å, is 0.13 Å less than that in the more oxidized Y₇I₁₂Fe,⁵ whereas a difference of only 0.05 or 0.09 Å would be suggested by respective differences in metallic or crystal radii for Pr vs Y.^{18,19} The 2.75-Å value of *d*(Pr-Fe) is, as observed for other metal-centered clusters, strikingly less than in the binary intermetallics, viz., 3.095 Å (×12) in PrFe₂ (MgCu₂ type)²⁰ and ≥3.084 Å in Pr₂Fe₁₇, where there are also many Fe-Fe interactions.²¹

Direct electronic communication between the clusters seems improbable. The shortest distances across the Pr₂(Iⁱ)₂ rhombi that connect adjoining clusters in the layers, 4.505, 4.518, and 4.551 Å between pairs of Pr6, Pr5, and Pr2, respectively, correspond to minute and insignificant bond orders (0.01), and indeed, extended Hückel band calculations on this phase show negligible Pr-Pr overlap populations between clusters. Furthermore, the presence of the bridging iodine atoms in the Pr₂I₂ rhombi makes it difficult to interpret this as a Pr-Pr interaction rather than as a matrix or more extended effect. No further characterizations of Pr₁₂I₁₇Fe₂ have been attempted since a single-phase product is not yet available.

It should be mentioned that the known compound Gd₁₂I₁₇C₆ with the same M:X ratio features a completely different structure,⁹ cis- and trans-edge-sharing C₂-centered Gd₆ clusters in the form of zigzag chains. This raises an interesting question as to whether one might be able to isolate more reduced phases with M:X ratios even closer to 1:1 that are interconnected only by Xⁱ⁻ⁱ bridging halide atoms, approaching M₆Xⁱ⁻ⁱ_{12/2}, as alternatives to the several condensed chain or layered compounds known. Part of this must depend on the relative magnitudes of Pr-Pr vs Pr-I bond strengths.

The structure of Pr₁₂I₁₇Fe₂ once again exhibits the beautiful structural diversity that can be achieved in cluster compounds where only the numbers of edge (12) and vertex (6) bonded halogen are constraints in the connectivities.

Acknowledgment. This research was supported by the National Science Foundation, Solid State Chemistry, via Grants DMR-8902954 and -9207361 and was carried out in facilities of the Ames Laboratory, DOE.

Supplementary Material Available: Tables of data collection, refinement, and anisotropic displacement parameters (2 pages). Ordering information is given on any current masthead page.

(17) Llusar, R.; Corbett, J. D. *Inorg. Chem.* **1994**, *33*, 849.

(18) Pauling, L. *The Nature of the Chemical Bond*; Cornell University Press: Ithaca, NY, 1960; p 400.

(19) Shannon, R. P. *Acta Crystallogr.* **1976**, *A32*, 751.

(20) Tsvyashchenko, A. V.; Popova, S. V. *J. Less-Common Met.* **1985**, *108*, 115.

(21) Johnson, Q.; Wood, D. H.; Smith, G. S.; Ray, A. E. *Acta Crystallogr.* **1968**, *24B*, 274.